Local characterization of one-dimensional topologically ordered states

Jian Cui,[1,2] Luigi Amico,[3,4] Heng Fan,[1] Mile Gu,[4,5] Alioscia Hamma,[5,6] and Vlatko Vedral[4,7,8]

[1]*Institute of Physics, Chinese Academy of Sciences, Beijing 100190, People's Republic of China*

[2]*Freiburg Institute for Advanced Studies, Albert Ludwigs University of Freiburg, Albertstraße 19, 79104 Freiburg, Germany*

[3]*CNR-MATIS-IMM & Dipartimento di Fisica e Astronomia, Via S. Sofia 64, 95127 Catania, Italy*

[4]*Centre for Quantum Technologies, National University of Singapore, 3 Science Drive 2, Singapore 117543*

[5]*Center for Quantum Information, Institute for Interdisciplinary Information Sciences, Tsinghua University, Beijing 100084, People's Republic of China*

[6]*Perimeter Institute for Theoretical Physics, 31 Caroline Street N, Waterloo, Ontario, Canada N2L 2Y5*

[7]*Department of Physics, National University of Singapore, 2 Science Drive 3, Singapore 117542*

[8]*Department of Physics, University of Oxford, Clarendon Laboratory, Oxford OX1 3PU, United Kingdom*

(Received 15 April 2013; revised manuscript received 20 August 2013; published 11 September 2013)

We consider one-dimensional Hamiltonian systems whose ground states display symmetry-protected topological order. We show that ground states within the topological phase cannot be connected with each other through local operations and classical communication between a bipartition of the system. Our claim is demonstrated by analyzing the entanglement spectrum and Rényi entropies of different physical systems that provide examples for symmetry-protected topological phases. Specifically, we consider the spin-1/2 cluster-Ising model and a class of spin-1 models undergoing quantum phase transitions to the Haldane phase. Our results provide a probe for symmetry-protected topological order. Since the picture holds even at the system's *local scale*, our analysis can serve as a local experimental test for topological order.

DOI: 10.1103/PhysRevB.88.125117 PACS number(s): 03.67.Mn, 03.65.Vf, 05.50.+q, 75.10.−b

I. INTRODUCTION

Understanding topological order in extended systems is one of the major challenges in modern physics. Such an issue has immediate spinoff in condensed-matter physics,[1–4] but encompasses important aspects of quantum information as well.[5] Topologically ordered systems are (generically) gapped systems characterized by a specific degeneracy of the ground states.[4,6] The main attraction for quantum computation applications relies on the intrinsic robustness of such an order to external perturbations. Indeed, such a property is nothing but a rephrasing that no local-order parameter can be defined to characterize topologically ordered states (Elitzur theorem). This turns the main virtue of topological phases into a bottleneck because any search for such kind of order in actual physical systems is problematic. For the same reason, also more generic spin liquids, which may not be topologically ordered but nevertheless possess a gap and no local-order parameter, are long-sought states in condensed-matter physics nowadays.[3,7]

In the last few years, topological order in many-body systems has been studied using new approaches. It is believed that topological order can be characterized by the entanglement encoded in the states of the system.[8,9] More precisely, it is understood that such an order is related to a long-range entanglement, meaning that topological states cannot be adiabatically connected to nontopological ones using quantum circuits made of local (on the scale of the range of interaction in the underlying Hamiltonian) unitary gates.[10] Accordingly, any observable that, in principle, would be able to detect the topological order is intrinsically nonlocal.[7,11,12]

Here we push forward the idea that progress can be made regarding this aspect by analyzing how topologically ordered ground states change by varying the control parameter, within the quantum phase (instead of looking at a single copy of the ground state corresponding to a fixed value of the control parameter).[13] In particular, we explore whether the ground-state "evolution," by changing the Hamiltonian's control parameter p, can be achieved by local operations on the subsystems and classical interparty communication (LOCC), after having a bipartitioned system. The tool we exploit is provided by the differential local convertibility:[14] A given physical system is partitioned into two parties, A and B, limited to LOCC. We comment that the notion of locality that we refer to does depend on the partition that has been employed; therefore, the LOCC can indeed involve a portion of the system that can be very nonlocal on the scale fixed by the interactions in the Hamiltonian. This should be contrasted with the protocols defining the topological order in terms of local unitary transformations mentioned above.[10]

Assuming that A and B can share an entangled state (ancilla), the differential local convertibility protocol can be feasibly expressed through a specific behavior of the Rényi entropies $S_\alpha \doteq \frac{1}{1-\alpha}\log \mathrm{Tr}\,\rho^\alpha$. The differential convertibility holds if and only if $\partial_p S_\alpha \geqslant 0$, $\forall\alpha$ or $\partial_p S_\alpha \leqslant 0$, $\forall\alpha$.[14] In the present paper, we will be using the latter characterization. Such an approach was first discussed in the realm of quantum critical phenomena in Ref. 15. In particular, we note that paramagnets and phases with nonvanishing local-order parameters are indeed locally convertible.[16]

In this paper, we focus on spin systems in one spatial dimension (1D), where topological order is protected by the symmetry of the system.[17] We shall see that such symmetry-protected topological phases are not convertible. We shall see that such property holds on spatial scales that are smaller than the correlation length of the system.

To address the question, we refer to specific spin systems providing paradigmatic examples in this context. First we will consider the cluster-Ising model[18,19] (see also Refs. 20 and 21).

The physical platform for that is provided by cold atoms in a triangular optical lattice.[22,23] The model is particularly interesting in quantum information since it describes how the 1D-cluster states are quenched by a qubit-qubit exchange interaction.[24] Our second example is the λ-D model, which is a well-known model for studying the Haldane order in 1D quantum magnets.[25,26] Quantum computation protocols based on Haldane-type states have been provided in Ref. 27.

The main numerical tool for the analysis is the density-matrix renormalization group (DMRG) technique with matrix product states (MPS) variational ansatz.[28] For both the cluster-Ising and the λ-D models, we analyze Rényi entropies, entanglement spectrum, and differential local convertibility.

In Secs. II and III, the differential local convertibility of the cluster-Ising and λ-D models will be analyzed. The scenario emerging from our study will be discussed in Sec. IV. In Appendices A and B, we discuss edge states, correlation lengths, and string order parameters of the models we deal with. The differential local convertibility for partition sizes larger than the correlation length of the system will be discussed in Appendix C. In Appendix D, we discuss the Rényi entropy in the large α limit.

II. THE CLUSTER-ISING MODEL

The Hamiltonian we consider is

$$H(g) = -\sum_{j=1}^{N} \sigma_{j-1}^{x}\sigma_{j}^{z}\sigma_{j+1}^{x} + g\sum_{j=1}^{N} \sigma_{j}^{y}\sigma_{j+1}^{y}, \qquad (1)$$

where $\sigma_i^{\alpha}, \alpha = x, y, z$, are the Pauli matrices and, except where otherwise stated, we take open boundary conditions $\sigma_{N+1}^{\alpha} = \sigma_0^{\alpha} = 0$. The phase diagram of (A1) has been investigated in Refs. 18 and 19. For large g, the system is an antiferromagnet with local-order parameter. For $g = 0$, the ground state is a cluster state. It results in a correlation pattern characterizing the cluster state that is robust up to a critical value of the control parameter, meaningfully defining a "cluster phase" with vanishing order parameter and string order.[18,19] Without symmetry, the cluster phase is a (nontopological) quantum spin liquid, since there is a gap and no symmetry is spontaneously broken. Protected by a $Z_2 \times Z_2$ symmetry, the cluster phase is characterized by a topological fourfold ground-state degeneracy, reflecting the existence of the edge states (see Appendix A).[18,29] In the DMRG, we resolve the ground-state degeneracy by adding a small perturbation, $\sigma_1^x\sigma_2^z \pm \sigma_{N-1}^z\sigma_N^x$, to the Hamiltonian.

We find that the symmetric partition $A|A$ displays local convertibility, as shown in Figs. 1(a1) and 1(a2). This is, indeed, a fine-tuned phenomenon since the cluster phase results are nonlocally convertible, for a generic block of spins, both of the type $A|B$ and the $B|A|B$; see Fig. 1. We remark that such a property holds even for size region A smaller than the correlation length (see Appendix C for other partitions). Indeed, the entanglement spectrum is doubly degenerate in the entire cluster phase, as far as the size of the blocks A and B are larger than the correlation length. In contrast, the antiferromagnet is locally convertible, with a nondegenerate entanglement spectrum.

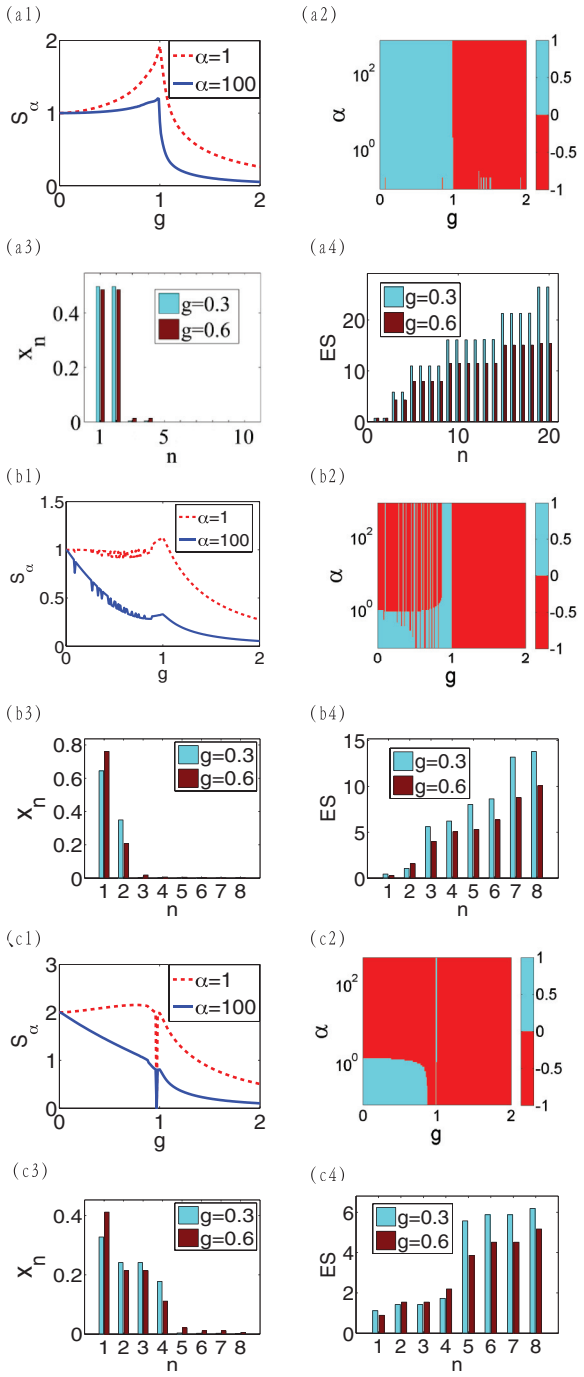

FIG. 1. (Color online) The local convertibility and the entanglement spectrum of the cluster-Ising model given by Eq. (A1). We characterize the differential local convertibility in terms of the slopes of the Rényi entropies. (a) Bipartition $A|A$, $A = 50$. There is differential local convertibility throughout the two different phases because for fixed g, $\partial_g S_\alpha$ does not change sign with α. (b) Bipartition $A|B$, $A = 3$, $B = 97$. (c) $A|B|C$, being one blocks $A \cup C$ with $A = 48$, $C = 49$, and $B = 3$. In all of these cases, $\partial_g S_\alpha$ changes sign. (a3), (a4), (b3), (b4), (c3), (c4) The large and the small eigenvalues of reduced density matrix x_n, respectively; $ES \doteq \{-\log x_n\}$. In convertible phases, we observe that the change in the largest eigenvalues is "faster" than the rate at which the smallest eigenvalues are populated. In contrast, the nondifferential local convertibility arises because the sharpening of the first part of the spectrum is overcompensated by the increasing of the smallest x_n.

III. THE λ-D MODEL

In this section, we study the local convertibility of the λ-D model Hamiltonian describing an interacting spin-1 chain with a single ion anisotropy,

$$H = \sum_i \left[\left(S_i^x S_{i+1}^x + S_i^y S_{i+1}^y \right) + \lambda S_i^z S_{i+1}^z + D \left(S_i^z \right)^2 \right], \quad (2)$$

where S^u, $u = \{x, y, z\}$, are spin-1 operators: $S^z|\pm\rangle = \pm|\pm\rangle$ and $S^z|0\rangle = 0$. The Hamiltonian above enjoys several symmetries: the well-known $Z_2 \times Z_2$ and the link inversion symmetry $S_j^u \to S_{-j+1}^u$ (see Appendix B). The phase diagram has been investigated by many authors[30–32] (see Appendix B). Here we consider $\lambda > 0$. For small/large D and fixed λ, the system is in a polarized state along $|+\rangle \pm |-\rangle$ or $|0\rangle$, respectively. For large λ and fixed D, the state displays antiferromagnetic order. At intermediate D and λ, the state is a "diluted antiferromagnet" with strong quantum fluctuations, defining the Haldane phase, lacking of local order parameters and string order. For open boundary conditions (which we apply in the present paper), the Haldane ground state displays a fourfold degeneracy that cannot be lifted without breaking the aforementioned symmetry of the Hamiltonian. This is the core mechanism defining the Haldane phase as a symmetry-protected topological-ordered phase.[33,34] Without symmetry, the ground state is gapped and no symmetry is spontaneously broken, making the Haldane phase a quantum spin liquid.

We sweep through the phase diagram in the following two ways: (1) Fix $\lambda = 1$ and change D; the Haldane phase is approximately located in the range $-0.4 \lesssim D \lesssim 0.8$. (2) Fix $D = 0$, varying on λ; the Haldane phase is located in the range $0 \lesssim \lambda \lesssim 1.1$ (see Fig. 2).

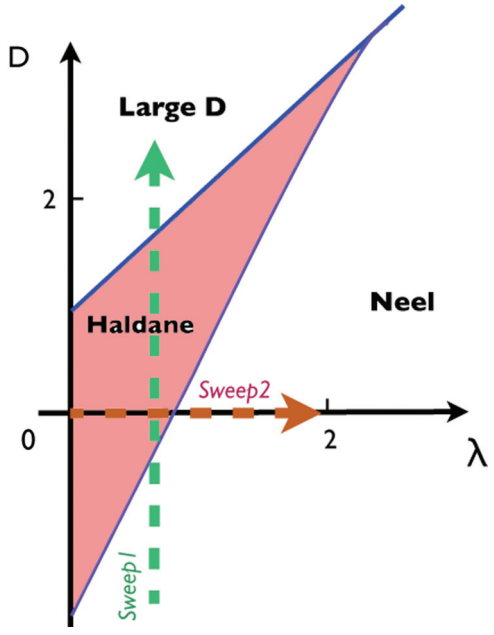

FIG. 2. (Color online) We sweep through the phase diagram in the following two ways: (1) Fix $\lambda = 1$ and change D; the Haldane phase is approximately located in the range $-0.4 \lesssim D \lesssim 0.8$. (2) Fix $D = 0$, varying on λ; the Haldane phase is located in the range $0 \lesssim \lambda \lesssim 1.1$.

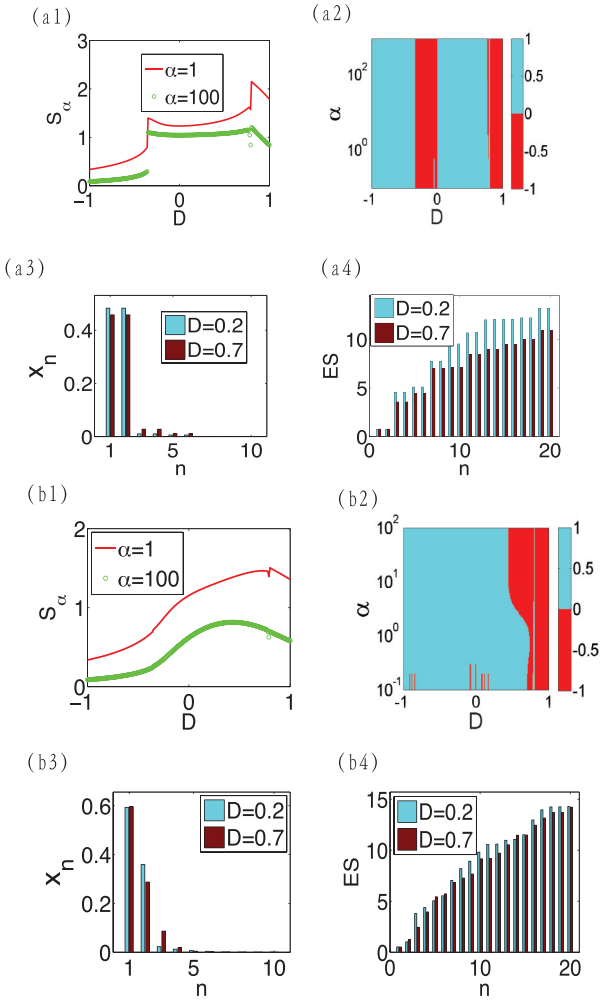

FIG. 3. (Color online) The local convertibility for the partition $A|B$. The sweep (1) through the λ-D phase diagram is considered (see also Appendix B for the schematic phase diagram). The upper panel displays the results for the symmetric case $A|A$. The bottom panel refers to the antisymmetric case $A = 96$, $B = 4$. (a1), (b1) The Rényi entropies. (a2), (b2) The sign distributions of the derivatives of the Rényi entropies. (a3), (a4), (b3), (b4) Eigenvalues of reduced density matrix x_n and the entanglement spectrum as in Fig. 1. The features of differential local convertibility are characterized by the slopes of the Rényi entropies and correspond to specific features of the entanglement spectrum, as explained in Fig. 1.

We analyzed all four states separately adding the perturbation to the Hamiltonian $\sim(S_1^z \pm S_N^z)$ with a small coupling constant.

We find that the Néel, ferromagnetic, and the large D phases are locally convertible [see Figs. 3(a1) and 3(a2)]. Consistent with Ref. 35, all of the Haldane ground states are characterized by a doubly degenerate entanglement spectrum for the symmetric $A|B$ partitions with $A = B$, for both sweep ways [Figs. 3(a3) and 3(a4)] [see (Ref. 36) for a recent progress on the understanding of double degenerate entanglement spectrum]. Such a property is not recovered both in the cases of asymmetric $A|B$ and $A|B|A$ partitions, where the entanglement spectrum is not found doubly degenerate

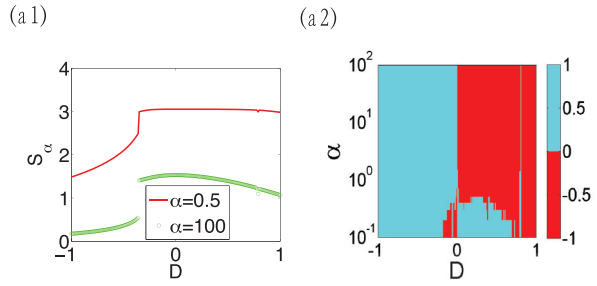

FIG. 4. (Color online) Sweep (1) through the λ-D model: $\lambda = 1$, $D \in \{-1,1\}$ (the schematic phase diagram is reported in Appendix B). The sign distribution of the derivative of the Rényi entropies $\partial_D S_\alpha$ for partitions $A|B|A$, $A = 48$ and $B = 4$ ($N = 100$) presented in (a2). The features of differential local convertibility are characterized by the slopes of the Rényi entropies and correspond to specific features of the entanglement spectrum, as explained in Fig. 1. The S_α are presented in (a1) for $\alpha = 0.5, 100$ decreasing from top to bottom. All such quantities are calculated for the ground state in the $S_z^{\text{tot}} = 1$ sector.

[Figs. 3(b3) and 3(b4)]. See Ref. 37 for the analysis of the entanglement spectrum close to the quantum phase transitions.

We find that the Haldane phase is not locally convertible [see Figs. 3(b1), 3(b2), 4, and 5]. We remark that for both ways to partition the system, the non-local-convertibility phenomenon is found even in the case of sizes of B smaller than the correlation length ξ (see Appendix B for the behavior of ξ). As for the model given by Eq. (A1), we find that the symmetric bipartition $A = B$ displays local convertibility as a fine-tuned effect, which is broken for generic partitions (see Appendix C for other partitions).

IV. DISCUSSION

We explored quantitatively the notion of LOCC in 1D topologically ordered systems. In particular, we analyzed to what extent different ground states of the Hamiltonian within the topological phase can be "connected" by (entanglement-assisted) LOCC between two parts A, B in which the system has been divided. This issue is analyzed through the notion

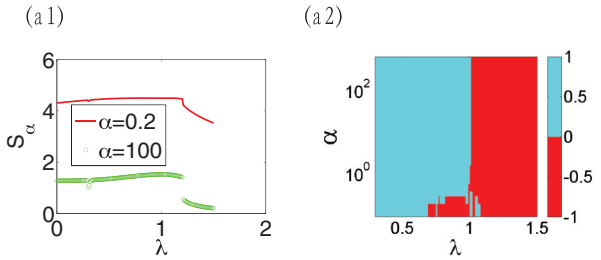

FIG. 5. (Color online) Sweep (2) through the λ-D model: $D = 0$, $\lambda \in \{0,1.5\}$ (see Fig. 2 for a schematic phase diagram). The sign distribution of the derivative of the Rényi entropies $\partial_\lambda S_\alpha$ for partitions $A|B|A$, $A = 48$ and $B = 4$ ($N = 100$), presented in (a2). The features of differential local convertibility are characterized by the slopes of the Rényi entropies and correspond to specific features of the entanglement spectrum, as explained in Fig. 1. The S_α are presented in (a1) for $\alpha = 100, 0.2$, increasing from bottom to top. All such quantities are calculated for the ground state in the $S_z^{\text{tot}} = 1$ sector.

of differential local convertibility that can be expressed in terms of the properties of the Rényi entropies. With this tool, we claim that progress can be made to detect quantum phases without a local-order parameter (contributing to the long-sought hunt for quantum spin liquids, topologically ordered or not).[13]

In the present paper, we specifically analyzed the question as to whether this method is useful to study topologically ordered phases assisted by symmetries. To this end, we considered two very different models that are, at the same time, paradigmatic for the analysis of the notion of symmetry-protected topological order: the spin-1/2 cluster-Ising and the spin-1 λ-D chains. We find that the symmetry-protected topological phases are characterized by nonlocal convertibility, meaning that the Hamiltonian is more effective to drive the system through different topological states than LOCC between A and B. The phases with the local-order parameter turn out to be locally convertible.

The convertibility property is encoded in the specific response of the entanglement spectrum to the perturbation: The distribution of eigenvalues of the reduced density matrix gets sharpened in the most represented eigenvalues. This implies that high α-Rényi entropies can decrease; at the same time, the spectrum acquires a tail made of small eigenvalues because more states are involved by increasing the correlation length [see Figs. 1(c2), 1(c3) and Figs. 3(b2), 3(b3)]. The local convertibility is achieved when the sharpening is compensated by the tail of the distribution (see Figs. 1 and 3).[38] We note the counterintuitive phenomenon in which some quantum correlations encoded in S_α, for certain α, decrease, in spite of the increase in correlation length (see Appendix B). Indeed, a similar phenomenon was discovered in the two-dimensional (2D) toric code,[13] corroborating the scenario described in the present paper. In particular, it was noticed that despite being nontopological ordered, certain spin liquids are also nonlocally convertible for specific perturbations. Therefore, an interesting question arises concerning the "stability" of the local convertibility by changing the perturbation. We observe, on the other hand, that spin liquids with some symmetry protection are, indeed, stable, spanning a well-defined quantum phase, distinct from a paramagnet. The results of the present paper indicate that the same symmetry protection is also able to protect their nonlocal convertibility.

The nonlocal convertibility occurs in the topological phases even for subsystem sizes *smaller than the correlation length* of the system (see Appendices B and A for the behavior of ξ in the models we analyzed); the degeneracy in the entanglement spectrum, in contrast, is exhibited when the aforementioned size is much larger than ξ. Clearly, this paves the way to experimental tests through local measures on a spatial region of sizes made of few spins, with the assistance of the protocols to address the Rényi entropies provided recently.[39] Incidentally, we note that for the symmetric partition $A|B$, there is differential local convertibility, but this is a fine-tuned effect that disappears if the two blocks have different size; see Figs. 1 and 3. Ultimately, the size and type of subsystems A and B on which the differential local convertibility is displayed depend on the recombination of the edge states that form at edges of the bipartition (see Ref. 16 for an extensive discussion of such edge-state recombination phenomenon). With our results,

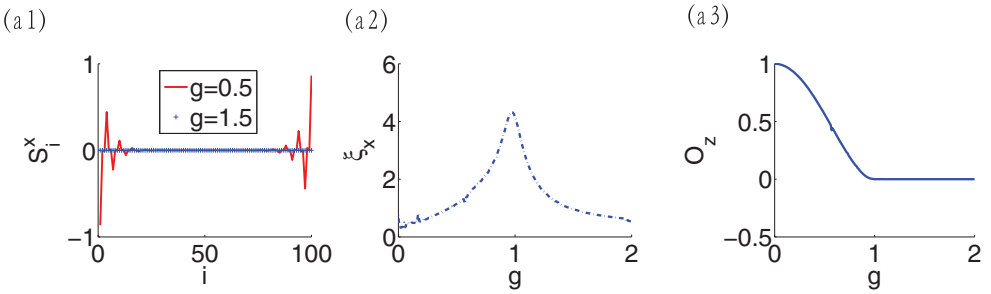

FIG. 6. (Color online) The edge state, correlation length, and string order parameter of the cluster-Ising model. (a1) shows that there is an edge state in the cluster phase, whereas there is no edge state in the Ising antiferromagnetic phase. (a2) shows the correlation length of $\langle\sigma_n\sigma_{n+3}\rangle - \langle\sigma_n\rangle\langle\sigma_{n+3}\rangle$ displaying a critical behavior. (a3) The string order parameter $O_z = (-)^{N-2}\langle\sigma_1^y \prod_{j=1}^{N-1}\sigma_j^z\sigma_N^y\rangle$.

we can claim that the local convertibility can characterize the phase, independently of the way the system is partitioned. We believe that such a scenario provides valuable assistance to standard routes in experimental solid-state physics to disclose topological order in the system.

Our work opens several questions that will be the subject of future investigation. In particular, it is important to establish the precise relation between the ground-state adiabatic evolution and the differential local convertibility.[10] Another interesting question is the role of differential convertibility in 2D symmetry-protected topologically ordered systems, such as topological insulators.

ACKNOWLEDGMENTS

We thank M. C. Banuls, L. Cincio, F. Franchini, T. Shi, H. H. Tu, S. Santra, and P. Zanardi for discussions. This work was supported in part by the National Basic Research Program of China Grants No. 2011CBA00300 and No. 2011CBA00301, the National Natural Science Foundation of China Grants No. 61073174, No. 61033001, No. 61061130540, and No. 11175248, and the 973 program (Grant No. 2010CB922904). Research at the Perimeter Institute for Theoretical Physics is supported in part by the Government of Canada through NSERC and by the Province of Ontario through MRI.

APPENDIX A: STRING ORDER PARAMETERS, CORRELATION LENGTH, AND EDGE STATES IN CLUSTER-ISING MODEL

The cluster-Ising Hamiltonian is

$$H(g) = -\sum_{j=1}^{N}\sigma_{j-1}^x\sigma_j^z\sigma_{j+1}^x + g\sum_{j=1}^{N}\sigma_j^y\sigma_{j+1}^y. \qquad \text{(A1)}$$

Without symmetry, the cluster phase in the cluster-Ising model is a (nontopological) quantum spin liquid, since there is a gap and no symmetry is spontaneously broken. Protected by a $Z_2 \times Z_2$ symmetry, the cluster phase is characterized by a topological fourfold ground-state degeneracy in open boundary conditions, reflecting the existence of the edge states. Such a degeneracy fans out from $g = 0$, where four Majorana fermions are left free at the free ends of the chain. The cluster phase can be characterized via a string order. The two phases are separated by a continuous quantum phase transition with central charge $c = 3/2$. Indeed, the Hamiltonian (A1) is equivalent to three decoupled Ising chains.[18,19]

After the Jordan-Wigner transformation $\sigma_k^+ = c_k^\dagger\prod_{j<k}\sigma_j^z$, $\sigma_k^- = c_k\prod_{j<k}\sigma_j^z$, $\sigma_k^z = 2c_k^\dagger c_k - 1$, the Hamiltonian of the cluster-Ising model can be written as

$$H(g) = -i\sum_k\left[f_k^{(2)}f_{k+2}^{(1)} - gf_k^{(1)}f_{k+1}^{(2)}\right], \qquad \text{(A2)}$$

where $f_k^{(1)} = c_k + c_k^\dagger$ and $f_k^{(2)} = -i(c_k - c_k^\dagger)$ are two different Majorana fermion operators.

Although local-order parameters do not exist to characterize the topological phase, the topological order in the cluster-Ising model (see Fig. 6) can be detected by the edge states [Fig. 6(a1)] and string order parameters [Fig. 6(a3)].

APPENDIX B: STRING ORDER PARAMETERS, CORRELATION LENGTH, AND EDGE STATES IN λ-D MODEL

The λ-D Hamiltonian is

$$H = \sum_i\left[\left(S_i^xS_{i+1}^x + S_i^yS_{i+1}^y\right) + \lambda S_i^zS_{i+1}^z + D\left(S_i^z\right)^2\right]. \qquad \text{(B1)}$$

The Hamiltonian above enjoys several symmetries, including the time reversal $S^{x,y,z} \to -S^{x,y,z}$, parity $S^{x,y} \to -S^{x,y}$, $S^z \to S^z$ generating $Z_2 \times Z_2$, and the link inversion symmetry $S_j^u \to S_{-j+1}^u$. For small/large D and fixed λ, the system is in a polarized state along $|+\rangle \pm |-\rangle$ or $|0\rangle$, respectively. For large λ and fixed D, the state displays antiferromagnetic order. At

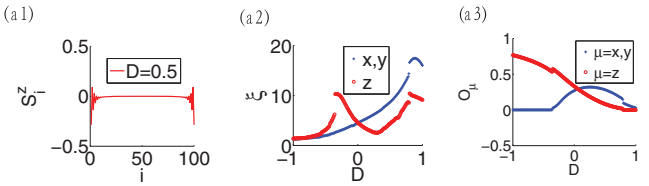

FIG. 7. (Color online) The edge states, correlation lengths, and string order parameters of the λ-D model. The sweep (1) through the λ-D phase diagram is considered (see text). (a1) The Haldane phase edge states; we do not find edge states in the other phases. (a2) The string order parameters $O_u = (-)^{N-2}\langle S_1^u\prod_{j=1}^{N-1}e^{i\pi S_j^u}S_N^u\rangle$. (a3) The correlation length of $\langle S_j^uS_{j+n}^u\rangle - \langle S_j^u\rangle\langle S_{j+n}^u\rangle$.

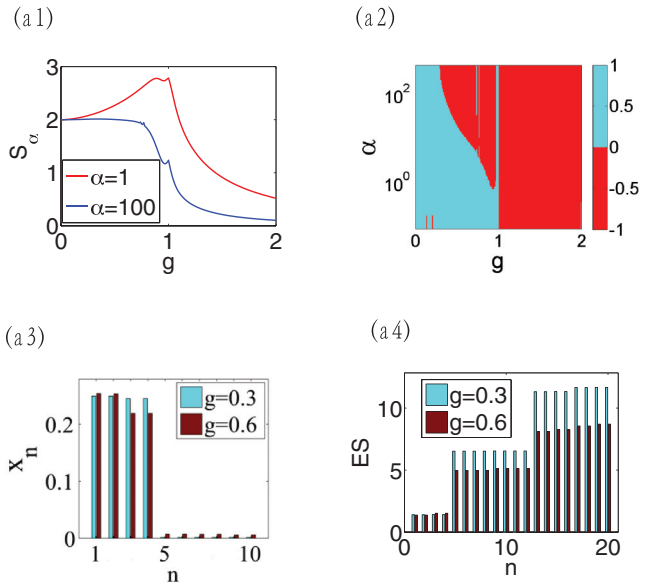

FIG. 8. (Color online) The local convertibility and the entanglement spectrum of the cluster-Ising model with bipartition 45|10|45. We characterize the differential local convertibility in terms of the slopes of the Rényi entropies. $\partial_g S_\alpha$ changes sign in the cluster phase. (a3), (a4) The large and the small eigenvalues of reduced density matrix x_n, respectively; $ES \doteq \{-\log x_n\}$. In convertible phases, we observe that the change in the largest eigenvalues is "faster" than the rate at which the smallest eigenvalues are populated. In contrast, the nondifferential local convertibility arises because the sharpening of the first part of the spectrum is overcompensated by the increasing of the smallest x_n.

intermediate D and λ, the state is a "diluted antiferromagnet" with strong quantum fluctuations, defining the Haldane phase. There are also no local-order parameters to characterize the Haldane phase in the λ-D model. With symmetry protection, the topological order in the Haldane phase can be detected by the edge states and string order parameters defined in Fig. 7 (see Ref. 40). Without symmetry, the ground state is gapped and no symmetry is spontaneously broken, making the

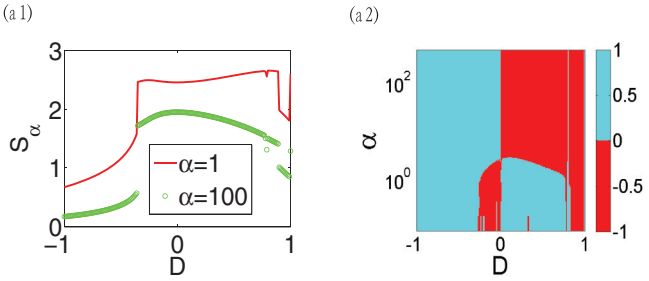

FIG. 9. (Color online) Sweep (1) through the λ-D model: $\lambda = 1$, $D \in \{-1,1\}$. The sign distribution of the derivative convertibility of the Rényi entropies $\partial_D S_\alpha$ for partitions $A|B|A$, $A = 45$ and $B = 10$ ($N = 100$), presented in (a2). The features of differential local convertibility are characterized by the slopes of the Rényi entropies and correspond to specific features of the entanglement spectrum, as explained in Fig. 1. The S_α are presented in (a1) for $\alpha = 1, 100$ decreasing from top to bottom. All such quantities are calculated for the ground state in $S_z^{\text{tot}} = 1$ sector.

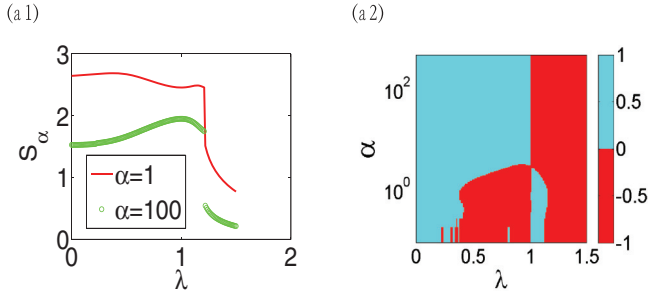

FIG. 10. (Color online) Sweep (2) through the λ-D model: $D = 0$, $\lambda \in \{0, 1.5\}$. The sign distribution of the derivative of the Rényi entropies $\partial_\lambda S_\alpha$ for partitions $A|B|A$, $A = 45$ and $B = 10$ ($N = 100$), presented in (a2). The features of differential local convertibility are characterized by the slopes of the Rényi entropies and correspond to specific features of the entanglement spectrum, as explained in Fig. 1. The S_α are presented in (a1) for $\alpha = 100, 1$ increasing from bottom to top. All such quantities are calculated for the ground state in the $S_z^{\text{tot}} = 1$ sector.

Haldane phase a quantum spin liquid. In Fig. 2, we display the schematic phase diagram of the λ-D.

APPENDIX C: DIFFERENTIAL LOCAL CONVERTIBILITY WITH SUBSYSTEM SIZE LARGER THAN OR COMPARABLE TO THE CORRELATION LENGTH

In the main text, we have shown that the differential local convertibility method works well with subsystem size smaller than the correlation length. In this section, we present the results of subsystem size larger or equivalent to the correlation length (Figs. 8–10).

APPENDIX D: LARGE α LIMIT OF RÉNYI ENTROPY AND LOCAL CONVERTIBILITY

In the main text, by calculating the Rényi entropies with different parameters, we have generally shown that with fixed bipartition of the spin chain, states with symmetry-protected topological order cannot convert to each other via LOCC (assisted by entanglement), which is different from the statistics with local order. Indeed, to arrive at such a

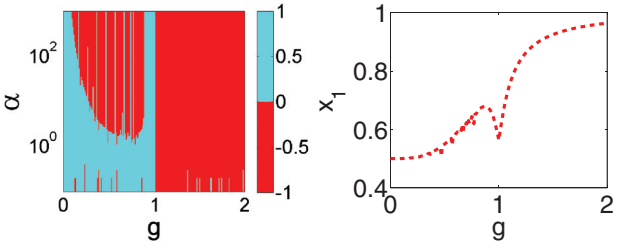

FIG. 11. (Color online) Cluster-Ising model, 90|10 bipartition. The left panel is the sign distribution of the Rényi entropy derivative which characterizes the region with nonlocal convertibility. The right panel is the largest eigenvalue, whose slope has the opposite sign with the Rényi entropy derivative in the large α limit. Comparing the two panels, we can see that our conclusion is still correct even if we go to infinite α.

conclusion rigorously, we have to calculate infinite Rényi entropies with α from 0 to ∞. From the definition of Rényi entropy $S_\alpha \doteq \frac{1}{1-\alpha} \log \mathrm{Tr}\, \rho^\alpha = \frac{1}{1-\alpha} \log \sum_i x_i^\alpha$, we can see that if we directly calculate the Rényi entropy with very large α numerically, then the numerator and denominator are both infinitely large such that a computer cannot give correct results. Therefore, in the $\alpha \to \infty$ limit, we can apply the l'Hôpital's rule to obtain $S_\infty = -\log x_1$, where x_1 is the largest eigenvalue. Notice that the S_α is a smooth and monotonic function of α, therefore we can arrive at the rigorous conclusion numerically by going to the numeric limit of α assisted with the verification by x_1; see Fig. 11.

[1] H. L. Stormer, D. C. Tsui, and A. C. Gossard, Rev. Mod. Phys. **71**, S298 (1999).

[2] M. Z. Hasan and C. L. Kane, Rev. Mod. Phys. **82**, 3045 (2010).

[3] S. Yan, D. A. Huse, and S. R. White, Science **332**, 1173 (2011).

[4] X.-G. Wen, *Quantum Field Theory of Many-body Systems* (Oxford University Press, Oxford, 2004).

[5] M. H. Freedman, A. Kitaev, and Z. Wang, Commun. Math. Phys. **227**, 587 (2002); C. Nayak, S. H. Simon, Ady Stern, M. Freedman, and S. Das Sarma, Rev. Mod. Phys. **80**, 1083 (2008).

[6] A. Y. Kitaev, Ann. Phys. (NY) **303**, 2 (2003).

[7] S. V. Isakov, M. B. Hastings, and R. G. Melko, Nat. Phys. **7**, 772 (2011).

[8] L. Amico, R. Fazio, A. Osterloh, and V. Vedral, Rev. Mod. Phys. **80**, 517 (2008).

[9] J. Eisert, M. Cramer, and M. B. Plenio, Rev. Mod. Phys. **82**, 277 (2010).

[10] Z. C. Gu and X. G. Wen, Phys. Rev. B **80**, 155131 (2009).

[11] A. Hamma, R. Ionicioiu, and P. Zanardi, Phys. Lett. A **337**, 22 (2005); Phys. Rev. A **71**, 022315 (2005); A. Kitaev and J. Preskill, Phys. Rev. Lett. **96**, 110404 (2006); M. Levin and X.-G. Wen, *ibid.* **96**, 110405 (2006).

[12] S. T. Flammia, A. Hamma, T. L. Hughes, and X.-G. Wen, Phys. Rev. Lett. **103**, 261601 (2009).

[13] A. Hamma, L. Cincio, S. Santra, P. Zanardi, and L. Amico, Phys. Rev. Lett. **110**, 210602 (2013).

[14] S. Turgut, J. Phys. A: Math. Theor. **40**, 12185 (2007); M. Klimesh, arXiv:0709.3680.

[15] J. Cui, M. Gu, L.-C. Kwek, M. F. Santos, H. Fan, and V. Vedral, Nat. Commun. **3**, 812 (2012).

[16] We remark that both the paramagnet and the ordered phases turn out to be locally convertible if symmetry breaking is taken into account. F. Franchini, J. Cui, L. Amico, H. Fan, M. Gu, V. E. Korepin, A. Hamma, L.-C. Kwek, and V. Vedral, arXiv:1306.6685.

[17] X. Chen, Z-C. Gu, and X-G. Wen, Phys. Rev. B **82**, 155138 (2010); **83**, 035107 (2011); **84**, 235128 (2011).

[18] W. Son, L. Amico, R. Fazio, A. Hamma, S. Pascazio, and V. Vedral, Europhys. Lett. **95**, 50001 (2011).

[19] P. Smacchia, L. Amico, P. Facchi, R. Fazio, G. Florio, S. Pascazio, and V. Vedral, Phys. Rev. A **84**, 022304 (2011).

[20] A. C. Doherty and S. D. Bartlett, Phys. Rev. Lett. **103**, 020506 (2009).

[21] S. O. Skrøvseth and S. D. Bartlett, Phys. Rev. A **80**, 022316 (2009).

[22] C. Becker, P. Soltan-Panahi, J. Kronjäger, S. Dörscher, K. Bongs, and K. Sengstock, New J. Phys. **12**, 065025 (2010).

[23] J. K. Pachos and M. B. Plenio, Phys. Rev. Lett. **93**, 056402 (2004).

[24] H. J. Briegel and R. Raussendorf, Phys. Rev. Lett. **86**, 910 (2001).

[25] F. D. M. Haldane, Phys. Rev. Lett. **61**, 1029 (1988).

[26] H. J. Mikeska and A. K. Kolezhuk, *Quantum Magnetism*, edited by U. Schollwöck, J. Richter, D. J. J. Farnell, and R. F. Bishop (Springer, Berlin, 2004).

[27] J. M. Renes, A. Miyake, G. K. Brennen, and S. D. Bartlett, New J. Phys. **15**, 025020 (2013).

[28] F. Verstraete, V. Murg, and J. I. Cirac, Adv. Phys. **2**, 143 (2008).

[29] W. Son, L. Amico, and V. Vedral, Quant. Inf. Proc. **11**, 1961 (2012).

[30] W. Chen, K. Hida, and B. C. Sanctuary, Phys. Rev. B **67**, 104401 (2003).

[31] C. Degli, Esposti Boschi, E. Ercolessi, and G. Morandi, in *Symmetries in Science XI* (Kluwer, Dordrecht, The Netherlands, 2004), pp. 145–173; arXiv:cond-mat/0309658.

[32] S. Hu, B. Normand, X. Wang, and L. Yu, Phys. Rev. B **84**, 220402(R) (2011).

[33] F. Pollmann, E. Berg, A. M. Turner, and M. Oshikawa, Phys. Rev. B **85**, 075125 (2012).

[34] S-P. Kou and X-G. Wen, Phys. Rev. B **80**, 224406 (2009).

[35] F. Pollmann, A. M. Turner, E. Berg, and M. Oshikawa, Phys. Rev. B **81**, 064439 (2010).

[36] W. Li, A. Weichselbaum, and J. von Delft, arXiv:1306.5671.

[37] L. Lepori, G. De Chiara, and A. Sanpera, Phys. Rev. B **87**, 235107 (2013); G. De Chiara, L. Lepori, M. Lewenstein, and A. Sanpera, Phys. Rev. Lett. **109**, 237208 (2012).

[38] We note that at very large α, the small eigenvalues produce a log divergence in S_α. The correct behavior can be achieved by analyzing x_1 (see Appendix D).

[39] A. J. Daley, H. Pichler, J. Schachenmayer, and P. Zoller, Phys. Rev. Lett. **109**, 020505 (2012); D. A. Abanin and E. Demler, *ibid.* **109**, 020504 (2012).

[40] E. Polizzi, F. Mila, and E. S. Sorensen, Phys. Rev. B **58**, 2407 (1998).